

Numerical Simulation of Optimal Source Temperature Distribution in PVT Method for SiC Single Crystals

Shota Tani^{a*}, Masato Urakami^b, Wataru Saito^c, Shin-Ichi Nishizawa^d

Kyushu University, Kasuga Koen 6-1, Kasuga, Fukuoka, Japan

^{a*}tani.shota.587@s.kyushu-u.ac.jp, ^burakami_masato@riam.kyushu-u.ac.jp,

^cwataru3.saito@riam.kyushu-u.ac.jp, ^ds.nishizawa@riam.kyushu-u.ac.jp

Keywords: virtual reactor, numerical simulation, physical vapor transport, recrystallization.

Abstract. In bulk SiC crystal growth using the PVT method, recrystallization within the source material leads to a decrease in growth rate and source utilization. In this study, numerical simulations were used to investigate the source temperature distribution and its effect on the growth rate and source utilization. Recrystallization in the upper and lower regions was considered separately. The results showed that reducing the source temperature gradient prevents recrystallization in the upper region, and a unidirectional gradient prevents recrystallization in the lower region, leading to higher growth rates and source utilization.

Introduction

The Physical Vapor Transport (PVT) method is widely used for growing bulk SiC crystals. In this method, SiC powder is used as the source, and the sublimation and temperature distribution in the source directly affects the crystal quality and manufacturing cost of SiC. The evolution of SiC powder during crystal growth has been studied in previous work using in-situ X-ray techniques [1, 2]. Generally, a moderate source temperature gradient enhances growth rate. However, when the temperature gradient is too high, a large amount of recrystallization occurs in the source [3, 4]. This problem reduces yield and growth rate, leading to high production costs. There have been many reports on studies of the SiC powder source in PVT growth [5,6,7,8]. However, few studies have focused on the optimization of source temperature distribution. This study uses numerical analysis with the STR software Virtual Reactor (VR) to examine the impact of recrystallization on growth rate and source utilization [9], and proposes an optimal source temperature distribution. In addition, the equilibrium vapor pressure dependent on temperature was used as a parameter to evaluate the source temperature distribution.

Optimal Source Temperature Distribution

Case 1: Conventional RF coil model.

In the PVT method, RF and resistance heating are employed as heating techniques for growing bulk SiC crystals. In Case1, the conventional RF coil model was used to examine the problem of recrystallization in the source. The modeling of the PVT furnace used is shown in Fig. 1. The model includes a graphite crucible, SiC powder, SiC seed, a seed holder, graphite felt insulation, and coils. Table 1 presents the physical properties of the materials used. A 4H polytype seed with a diameter of 120 mm was used. The growth was carried out under an Ar atmosphere at 1500 Pa, with the temperature controlled at 2250 °C at the center of the seed holder surface. The RF heating frequency was set to 10 kHz, and the heating power was calculated from the temperature and thermal properties of the structure. The growth time was set until the growth rate dropped below zero and the source was completely consumed, in order to calculate the source utilization. Growth steps were set at two-hour intervals, and the total crystal growth was calculated from the obtained results. Initial particle size in the source was set to 500 μm with a porosity of 0.6. Recrystallization is observed when the particle diameter exceeds this value. The utilization efficiency of the source was calculated as {[initial

source mass] – [residual source mass]} / [initial source mass]. The numerical modeling of the powder evolution is described in Reference [10].

In the high-temperature process of the PVT method, Lilov reported that the SiC reaction gas species are Si, Si₂C, and SiC₂. Below 2900 K, SiC₂ is the dominant species controlling the growth rate [11]. Therefore, not only the temperature but also the equilibrium vapor pressure of SiC₂ was considered for optimizing the source temperature distribution. The equilibrium vapor pressure values were calculated based on data traced from the graph published by Philippe Rocabois [12].

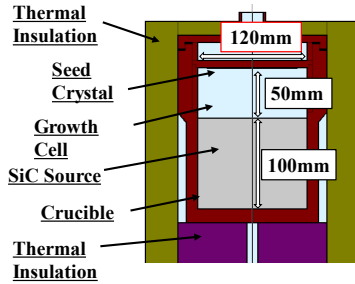


Fig. 1. Casel model: Structure of the Conventional RF heating Furnace.

Table 1. The physical parameters.

Components	Electric conductivity [S/m]	Thermal conductivity [W/(m×K)]	Density [kg/m ³]	Heat capacity [J/(kg×K)]	Emissivity
SiC seed crystal	1000	90	3220	920	0.9
SiC source Powder	4	10	1600	920	0.8
Graphite Crucible	1.6×10^5	30	1840	1300	0.8
Graphite insulation side	100	1.1	100	1000	0.8
Graphite insulation bottom	200	1.4	180	1000	0.8

Fig. 2 shows the temperature distribution in the crucible and the particle size distribution after 24 hours of crystal growth. Fig. 3 shows the temperature and the corresponding equilibrium vapor pressure of SiC₂ (P_{SiC₂}) along the center axis (0h) [11]. The 24-hour average growth rate was 219 μm/h, with a total growth of 2.59 cm. From Fig. 2, it can be especially confirmed that recrystallization occurs in both the upper and lower regions of the source. It is also observed in the middle region. Recrystallization occurs when the sublimated gas becomes supersaturated in the source. Here, the transport direction and flux of the sublimated gas are determined by the value of the equilibrium vapor pressure gradient dP_{SiC_2}/dy . Fig. 4 shows the equilibrium vapor pressure gradient, where negative values indicate gas flow toward the seed and positive values toward the bottom crucible. Differentiation was carried out using the finite difference method with $\Delta = 2$ mm. The source bottom is at $y = 15$, and below the seed crystal is at $y = 165$.

Recrystallization in the lower region occurs due to the temperature distribution created by RF coil heating, as the heat source is located at the crucible sidewall, leading to a gradual decrease in temperature toward the center. From Fig. 4, it can be seen that in the range of $y = 15$ –27, the vapor pressure gradient has positive values, causing gas transport toward the bottom crucible, resulting in supersaturation and recrystallization. Recrystallization in the upper region can be explained by the discontinuity of the equilibrium vapor pressure gradient at the source/gas interface. Fig. 4 shows that

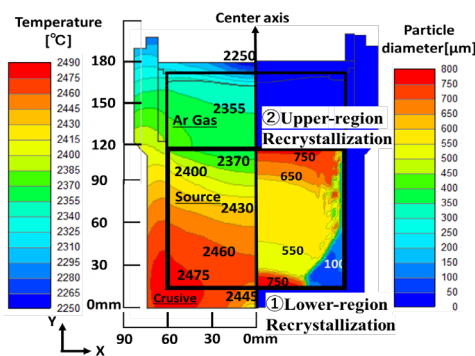


Fig. 2. Crucible temperature [°C] and particle size distribution [μm] (24h).

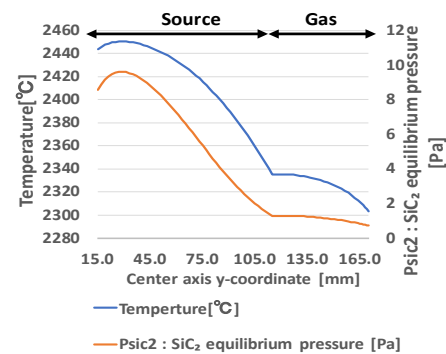


Fig. 3. Temperature [°C] and equilibrium vapor pressure of P_{SiC₂} [Pa] along the center axis (0h).

at the source–gas interface ($y = 115$), the vapor pressure gradient on the source side has a much larger negative value than that on the gas side. This gradient difference causes the sublimated gas to stagnate in the upper of the source, resulting in supersaturation and recrystallization. Similarly, recrystallization in the middle region occurs because, from $y = 27$, the vapor pressure gradient in the lower region becomes more negative than that in the upper region. In contrast to the vapor pressure gradient, the temperature gradient increases gradually in the source. This finding indicates that vapor pressure distribution, rather than temperature distribution, is the key parameter in determining recrystallization.

These results suggest that recrystallization occurs when the vapor pressure gradient dP_{SiC_2}/dy shifts from a large to a small negative value - in other words when the gradient of dP_{SiC_2}/dy ($=d^2P_{\text{SiC}_2}/dy^2$) becomes positive causing stagnation of sublimated gas transport. Therefore, Fig. 5 presents $d^2P_{\text{SiC}_2}/dy^2$ together with the SiC powder particle size growth rate [$\mu\text{m}/\text{h}$] at 0 h, indicating recrystallization in the source. This figure indicates that the particle size growth peaks at the source–gas interface ($y = 115$), where $d^2P_{\text{SiC}_2}/dy^2$ reaches a maximum value of 0.032 at the gas-side interface. In Case 3, $d^2P_{\text{SiC}_2}/dy^2$ at the source–gas interface was used as a parameter to study the effects of upper-region recrystallization on growth rate and source utilization. In Case 2, the lower temperature distribution was optimized.

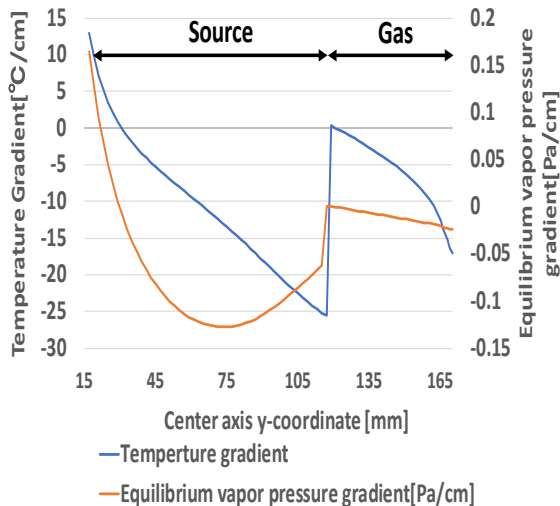


Fig. 4. Temperature gradient [$^{\circ}\text{C}/\text{cm}$] and equilibrium vapor pressure gradient dP_{SiC_2}/dy [Pa/cm] along the center axis.

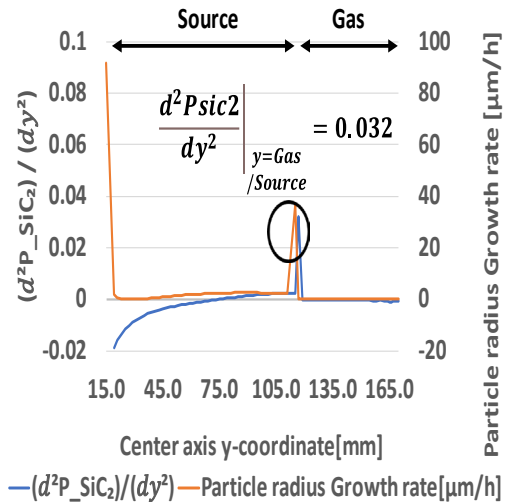


Fig. 5. Relationship between $d^2P_{\text{SiC}_2}/dy^2$ and Particle radius growth rate [$\mu\text{m}/\text{h}$] along the center axis.

Case 2: Optimizing the temperature in the lower.

In Case 2, the material at the bottom of the crucible was replaced with one with higher thermal conductivity to improve the temperature distribution in the lower part of the source. The analysis model and physical parameters are shown in Fig. 6 and Table 2. This material has fictitious properties to create an ideal temperature distribution. All other analysis conditions were the same as those used in Case 1. The 24-hour average growth rate was $217 \mu\text{m}/\text{h}$, the total growth was 3.17 cm . Compared with Case 1, the total growth increased by 0.58 cm , while the growth rate decreased by $2 \mu\text{m}/\text{h}$. Fig. 7 shows a unidirectional temperature gradient in the lower region of the source and no recrystallization, leading to improved source utilization.

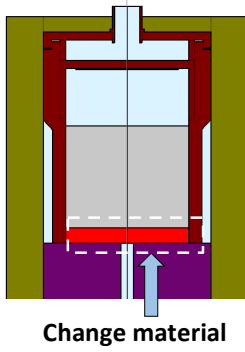


Fig. 6. Case 2 model: Change of bottom material.

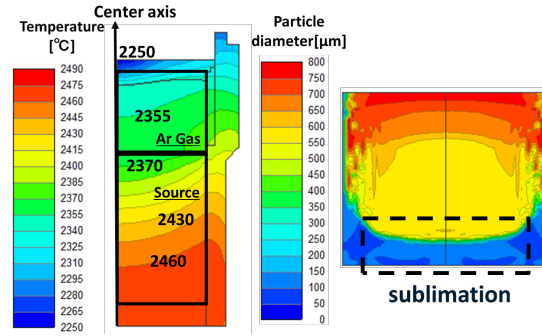


Fig. 7. Optimization of the lower source temperature distribution [°C] and particle size distribution [μm]. (24h).

Table 2. The physical parameters.

Parameter	Value
Electric conductivity	1.6×10^5 S/m
Thermal conductivity	500 W/(m * K)
Density	2200 kg/m
Heat capacity	1900 kg/m ³
Emissivity	0.8

The slight difference in growth rate is due to the lower maximum temperature in Case 2 than in Case 1, with the sublimated gas generated in the lower region consumed by recrystallization in the upper region. In practical induction heating, designing the lower temperature distribution shown in Fig. 7 is challenging. Therefore, it is important to lower the heat source and design the crucible so that the lower part is heated uniformly.

Case 3: Optimaizing the temperature in the upper.

In Case 3, we analyzed the influence of the $d^2P_{SiC_2}/dy^2$ at the source–gas interface on growth rate and source utilization by setting the source temperature difference in the range of $\Delta T_{source} = 4 \sim 50$ °C. The analysis model is shown in Fig. 8. This model differs from those used in Cases 1 and 2, with the temperature set at the boundary condition to realize an ideal temperature distribution, without using coils. The source sidewall was given a linear temperature boundary condition, and bottom was given a constant one. The crucible diameter was also reduced to 60 mm, and a flat temperature distribution was created by minimizing the lateral temperature gradient. Fig.9 shows the 0 h temperature and the 24 h particle size distribution, while Table 3 lists the temperatures and $d^2P_{SiC_2}/dy^2$ at the gas/source interface. As shown in Fig. 9,

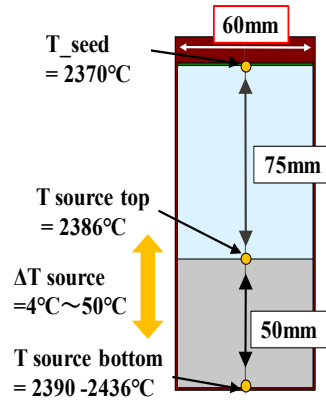


Fig. 8. Case3 model: The temperature was set at the boundary conditions for the ideal temperature distribution (no coils).

Table 3. Analysis Results of Case 3 model.

ΔT_{source} [°C]	T_{seed} [°C]	$T_{\text{source top}}$ [°C]	$T_{\text{source bottom}}$ [°C]	Total Growth [cm]	$\frac{d^2 P_{\text{SiC}_2}}{dy^2}$ _{y=Gas/Source}	Growth Rate [μm/h]	Utilization efficiency [%]
4	2370	2386	2390	2.49	0.010	164.4	91
10	2370	2386	2396	2.68	0.012	172.5	90
20	2370	2386	2406	2.79	0.017	173.7	83
30	2370	2386	2416	2.58	0.021	171.3	73
40	2370	2386	2426	2.23	0.027	165.8	44
50	2370	2386	2436	1.63	0.030	171.1	28

Growth Rate [μm/h] is the 24-hour average growth rate.; **Total growth [cm]** was calculated by summing the average growth rates until the source was fully consumed.; The pressure for all models was 1200 Pa.

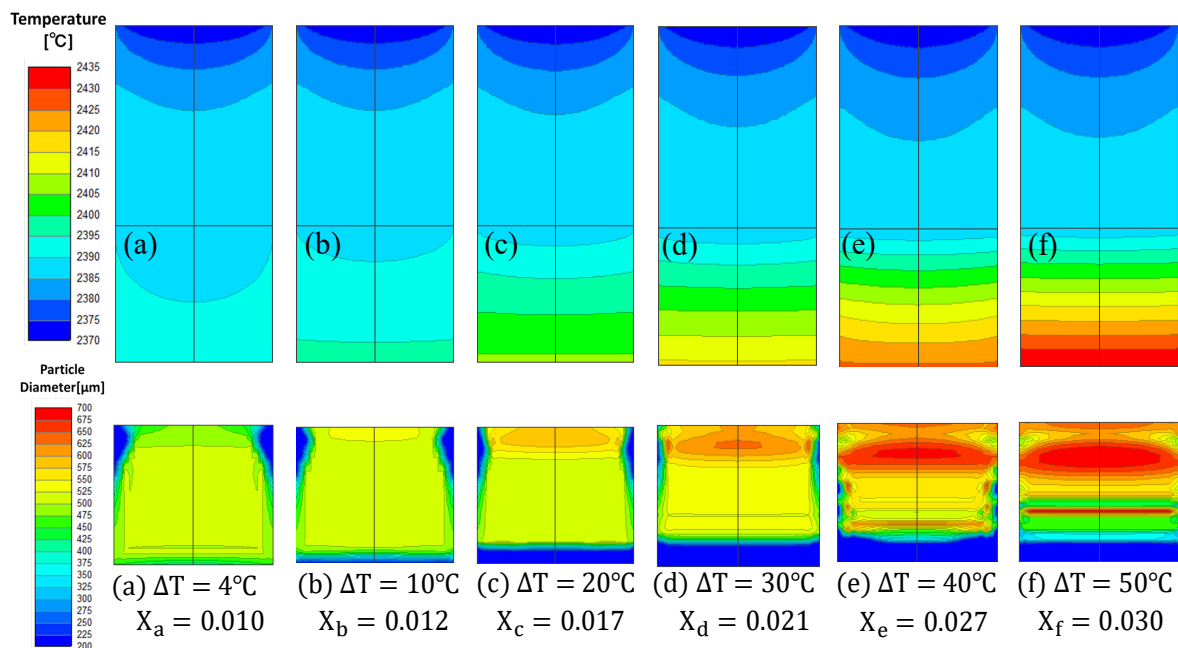


Fig. 9. Temperature distribution [°C] (0h) and particle size distribution [μm] (24h) for the Case 3 model. $\Delta T = \Delta T_{\text{source}}$: Temperature difference of the source along the center axis. $X_{a\sim f}$: $d^2P_{\text{SiC}_2}/dy^2$ at the source–gas interface.

a larger $d^2P_{\text{SiC}_2}/dy^2$ at the gas/source interface leads to greater particle size growth in the upper region. In addition, starting from $\Delta T = 30\text{ }^\circ\text{C}$ where $d^2P_{\text{SiC}_2}/dy^2 = 0.21$, it can be observed that the peak position of particle size gradually shifts toward the middle region, indicating that the sublimated gas is consumed before reaching the upper region. At $\Delta T_{\text{source}} = 4\text{ }^\circ\text{C}$, no recrystallization was observed in the source, and Fig. 10 shows the corresponding $d^2P_{\text{SiC}_2}/dy^2$ and the powder particle size growth rate [$\mu\text{m}/\text{h}$]. The source bottom is at $y = 2$, and below the seed crystal is at $y = 127$. These results also confirm that no recrystallization occurred throughout the entire source. Fig. 11 shows the relationship between the $d^2P_{\text{SiC}_2}/dy^2$ at the source–gas interface and the utilization efficiency and growth rate (24 h average). The growth rate reached their maximum at $d^2P_{\text{SiC}_2}/dy^2 = 0.017$ ($\Delta T_{\text{source}} = 20\text{ }^\circ\text{C}$), with values of $173\text{ }\mu\text{m}/\text{h}$. Thereafter, the growth rate showed a decreasing trend, which coincided with the timing when recrystallization began to shift downward to the middle region. At $d^2P_{\text{SiC}_2}/dy^2 = 0.030$ ($\Delta T_{\text{source}} = 50\text{ }^\circ\text{C}$), the growth rate temporarily increased but did not reach its maximum, and the utilization efficiency decreased to 28%. From these results, it was shown that the growth rate and source utilization efficiency can be maximized by setting $d^2P_{\text{SiC}_2}/dy^2$ at the source–gas interface. In practice, it is difficult to suppress the source temperature difference to $4\text{ }^\circ\text{C}$ or $10\text{ }^\circ\text{C}$ while maintaining a unidirectional source temperature distribution. Therefore, in thermal design for the PVT process, minimizing the source temperature difference is important. This allows the maximum source temperature to be reduced, which in turn helps lower power consumption and suppress the degradation of the crucible and insulation materials. If the growth rate needs to be increased, it is effective to maintain a low source temperature difference while either raising the overall temperature or enlarging the temperature difference in the gas region, which also helps reduce production costs. A more detailed analysis would require further examination of the computational model and its accuracy.

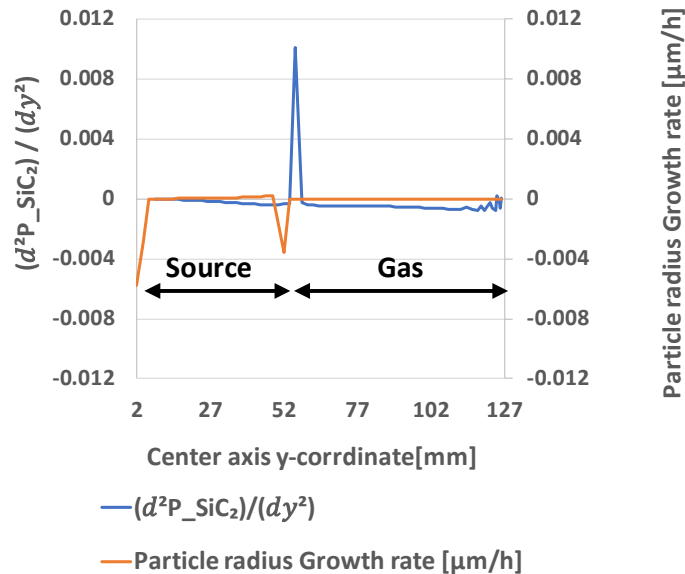


Fig. 10. Relationship between $d^2P_{\text{SiC}_2}/dy^2$ and Particle radius growth rate [$\mu\text{m}/\text{h}$] along the center axis. ($\Delta T_{\text{source}} = 4\text{ }^\circ\text{C}$).

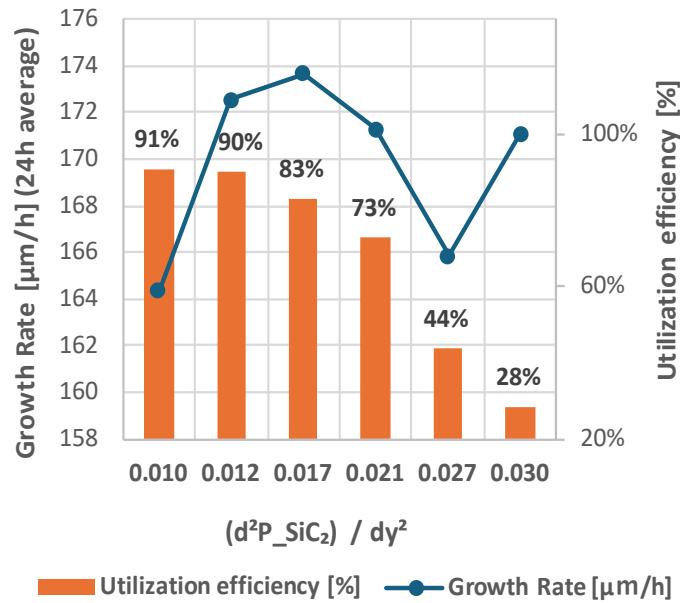


Fig. 11. Relationship between $d^2P_{SiC_2}/dy^2$ at the source–gas interface and the utilization efficiency and growth rate (24 h average).

Summary

The results revealed that the optimal temperature distribution suppresses recrystallization by minimizing and making the source temperature gradient unidirectional within the source. These improvements lead to higher growth rates and source utilization, which contribute to the reduction of wafer production costs.

References

- [1] P.J. Wellmann, M. Bickermann, D. Hofmann, L. Kadinski, M. Selder, T.L. Straubinger, A. Winnacker, In situ visualization and analysis of silicon carbide physical vapor transport growth using digital X-ray imaging, *J. Cryst. Growth* 216 (2000) 263-272.
- [2] Z.G. Herro, P.J. Wellmann, R. Püsche, M. Hundhausen, L. Ley, M. Maier, P. Masri, A. Winnacker, Investigation of mass transport during PVT growth of SiC by ¹³C labeling of source material, *J. Cryst. Growth* 258 (2003) 261-267.
- [3] X. Liu, B. Chen, L.X. Song, E.W. Shi, Z.Z. Chen, The behavior of powder sublimation in the long-term PVT growth of SiC crystals, *J. Cryst. Growth* 312 (2010) 1486-1490.
- [4] H. Li, X.L. Chen, D.Q. Ni, X. Wu, Factors affecting the graphitization behavior of the powder source during seeded sublimation growth of SiC bulk crystal, *J. Cryst. Growth* 258 (2003) 100-105.
- [5] D.S. Karpov, O.V. Bord, S.Yu. Karpov, A.I. Zhmakin, M.S. Ramm, Yu.N. Makarov, Mass transport and powder source evolution in sublimation growth of SiC bulk crystals, *Mater. Sci. Forum* 353-356 (2001) 37-40.
- [6] X. Wang, D. Cai, H. Zhang, Increase of SiC sublimation growth rate by optimizing of powder packaging, *J. Cryst. Growth* 305 (2007) 122-132.
- [7] H. Miao, G. Mi, Y. Liu, Effect of powder packing method on thermal field of SiC crystal grown by PVT method, *Ferroelectrics* 618 (2024) 2610-2621.

- [8] C. Zhou, Z. Lu, C. Li, Y. Lu, H. Li, L. Dong, S. Ke, S.Y. Tong, Optimization of SiC single crystal growth via numerical simulation: Enhanced mass transport with graphite ring and block design, *J. Cryst. Growth* 668 (2025) 128283.
- [9] M.V. Bogdanov, A.O. Galyukov, S.Yu. Karpov, A.V. Kulik, S.K. Kochuguev, D.Kh. Ofengeim, A.V. Tsiryulnikov, M.S. Ramm, A.I. Zhmakin, Yu.N. Makarov, Virtual reactor as a new tool for modeling and optimization of SiC bulk crystal growth, *J. Cryst. Growth* 225 (2001) 307-311. [9] theoretical analysis of the mass transport in powder charge.
- [10] A.V. Kulik, M.V. Bogdanov, S.Yu. Karpov, Y. Makarov, Theoretical analysis of the mass transport in the powder charge in long-term bulk SiC growth, *Mater. Sci. Forum* 457-460 (2004) 67-70.
- [11] S.K. Lilov, Study of the equilibrium processes in the gas phase during silicon carbide sublimation, *Mater. Sci. Eng. B* 21 (1993) 65-69.
- [12] P. Rocabois, C. Chatillon, C. Bernard, F. Genet, Thermodynamics of the Si-C system II. Mass spectrometric determination of the enthalpies of formation of molecules in the gaseous phase, *High Temp. High Press.* 27-28 (1996) 25-39.